

# Poroelastic Response of Shallow Crust Induced Seasonal Changes in Geohydrologic Parameters

Xin Liao<sup>1</sup>, Zhiqiang Fan<sup>2</sup>, Zhen-Yu Wang<sup>3</sup>, and Chunping Liu<sup>4</sup>

<sup>1</sup>Institute of Disaster Prevention; Hebei Key Laboratory of Earthquake Dynamics

<sup>2</sup>Northwestern Polytechnical University

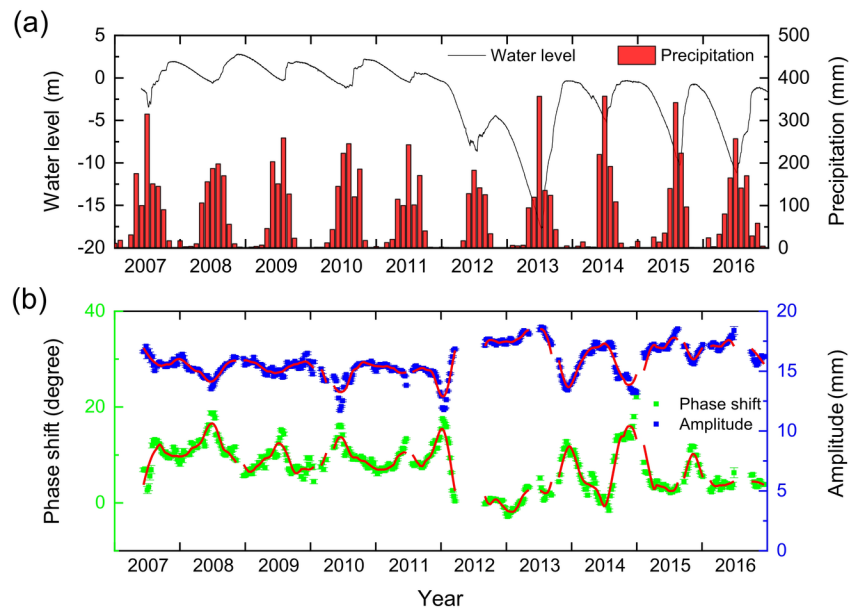
<sup>3</sup>Institute of Geophysics, China Earthquake Administration

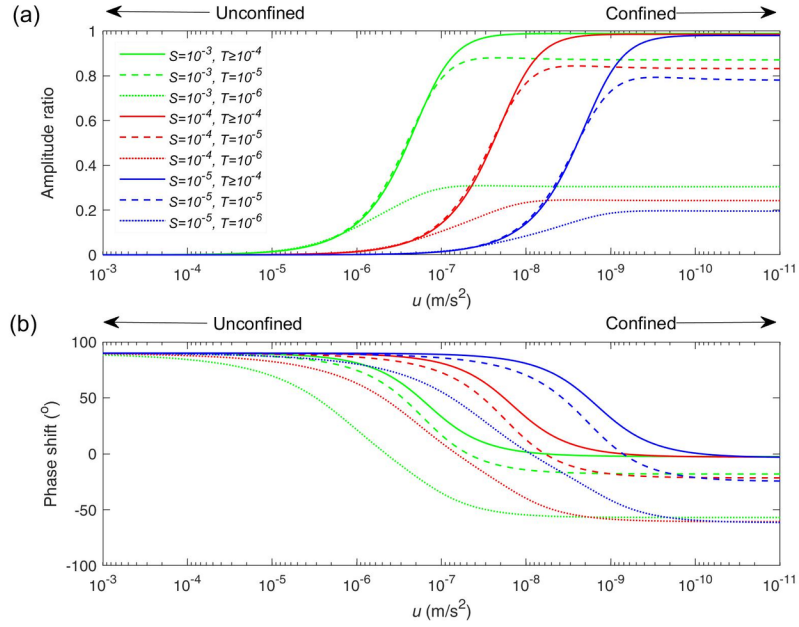
<sup>4</sup>Institute of Disaster Prevention

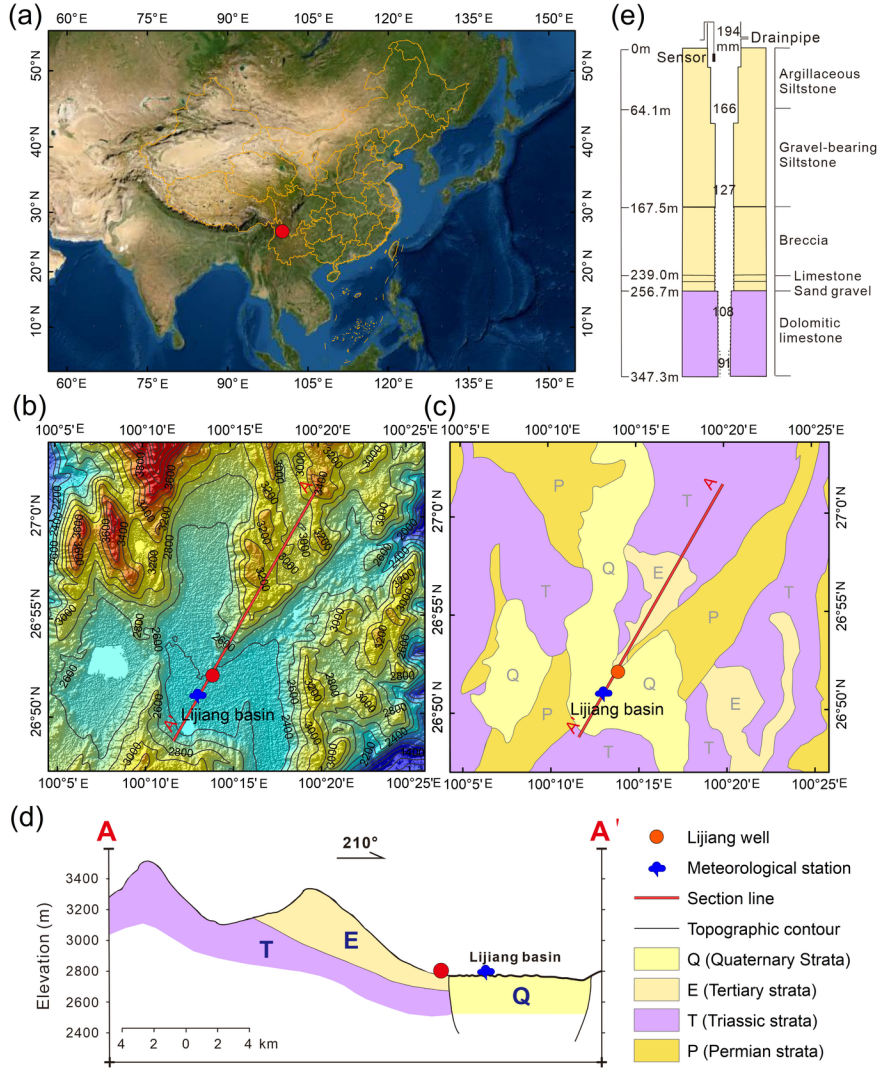
November 22, 2022

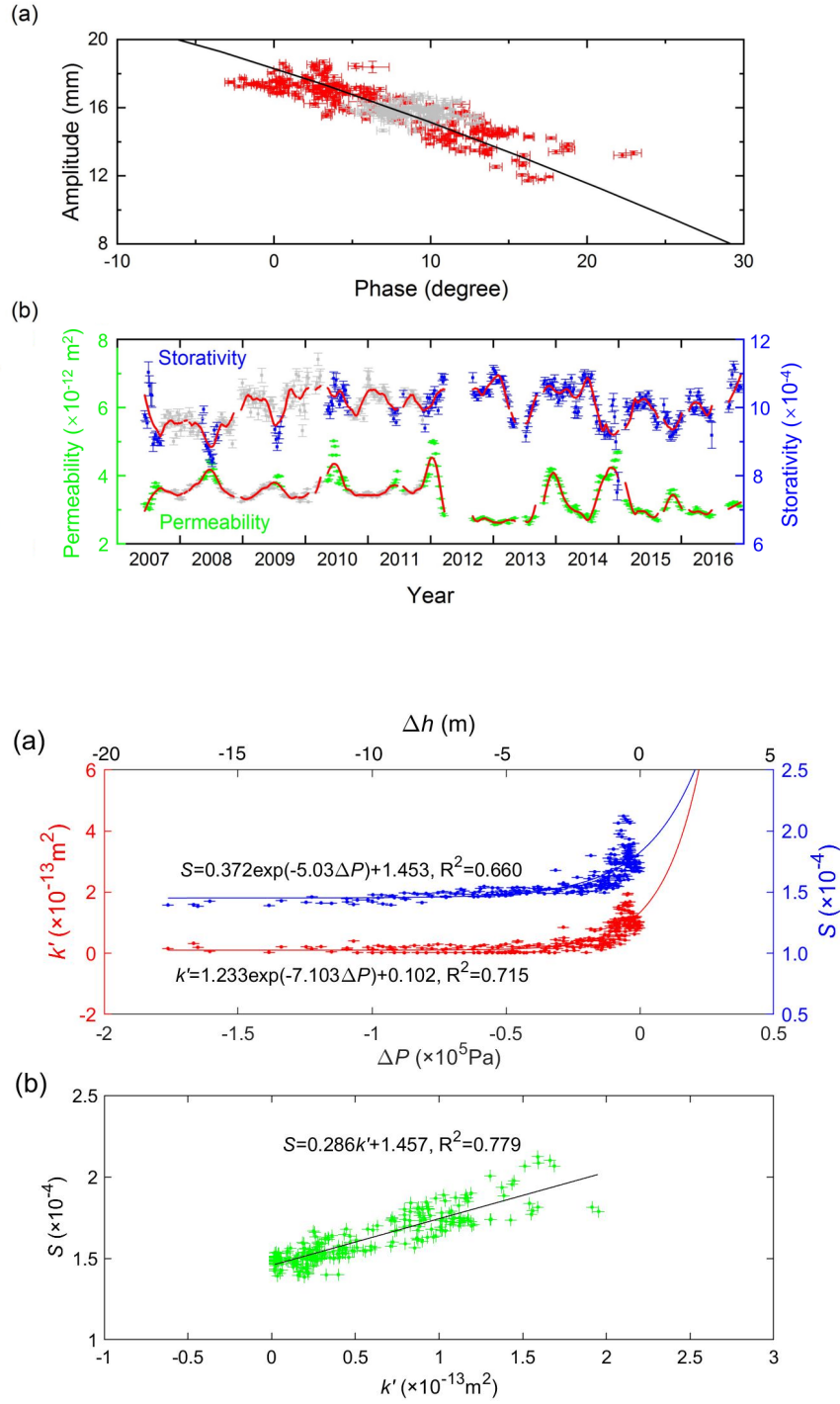
## Abstract

Quantitative evaluations of hydrological processes that induce changes in the geohydrologic parameters of groundwater systems are of great significance in subsurface hydrology. In this study, the tidal response of the water level in Lijiang well was considered as an indicator of the hydrological parameters, and the seasonal changes of the tidal response were investigated. The results suggested that the seasonal change of tidal response should be attributed to the seasonal changes in the geohydrologic parameters, which are caused by the opening/closing of pre-existing fractures or fracture aperture changes in the groundwater system, owing to regional precipitation recharge that produces a poroelastic response in the groundwater system. This suggests that the groundwater system in the shallow crust can be viewed as a natural positive feedback poroelastic-hydraulic coupled system during the hydrological processes. These findings may have far-reaching implications for the safety of the subsurface environment, ecosystem, and groundwater resources.









1 **Poroelastic Response of Shallow Crust Induced Seasonal Changes in**  
2 **Geohydrologic Parameters**

3 **Xin Liao<sup>1,2,\*</sup>, Zhiqiang Fan<sup>3</sup>, Zhen-Yu Wang<sup>4</sup>, Chun-Ping Liu<sup>1</sup>**

4 *1 School of Ecology and Environment, Institute of Disaster Prevention, Beijing 101601, China*

5 *2 Hebei Key Laboratory of Earthquake Dynamics, Institute of Disaster Prevention, Beijing*  
6 *101601, China*

7 *3 School of Mechanics, Civil Engineering and Architecture, Northwestern Polytechnical*  
8 *University, Xi'an 710072, China*

9 *4 Institute of Geophysics, China Earthquake Administration, Beijing 10081, China*

10 *\* Corresponding author: Xin Liao (liaoxin19851224@126.com)*

11

12 **Key Points:**

- 13 • The seasonal variation in geohydrologic parameters may be caused by changes in fracture  
14 apertures.
- 15 • Precipitation induced poroelastic response may change the geohydrologic parameters  
16 seasonally.
- 17 • Groundwater system is a poroelastic–hydraulic coupled system with positive feedback in  
18 the shallow crust.

19

20 **Plain Language Summary**

21 In this study, we investigated the unexpected seasonal changes in the tidal response of the water  
22 level observed in a well in Southwest China. We concluded that the seasonal geohydrologic  
23 parameters changes, including the changes in vertical permeability and storativity, can be  
24 explained by the fracture aperture changes in the groundwater system caused by regional  
25 precipitation recharge that induces pore pressure or effective stress changes. This suggests that  
26 the geohydrologic parameters are mutable properties during a hydrologic year, and that the  
27 groundwater system can be viewed as a positive feedback poroelastic–hydraulic coupled system  
28 during hydrological processes. Feedback from the seasonal geohydrologic parameters changes in  
29 the shallow crust may impact the subsurface system, including altering potential groundwater  
30 contamination risks, compromising the safety of nuclear waste storage, and influencing the  
31 diffusion and transport of subsurface contaminants.

## 32 **Abstract**

33 Quantitative evaluations of hydrological processes that induce changes in the geohydrologic  
34 parameters of groundwater systems are of great significance in subsurface hydrology. In this  
35 study, the tidal response of the water level in Lijiang well was considered as an indicator of the  
36 hydrological parameters, and the seasonal changes of the tidal response were investigated. The  
37 results suggested that the seasonal change of tidal response should be attributed to the seasonal  
38 changes in the geohydrologic parameters, which are caused by the opening/closing of pre-  
39 existing fractures or fracture aperture changes in the groundwater system, owing to regional  
40 precipitation recharge that produces a poroelastic response in the groundwater system. This

41 suggests that the groundwater system in the shallow crust can be viewed as a natural positive  
42 feedback poroelastic–hydraulic coupled system during the hydrological processes. These  
43 findings may have far-reaching implications for the safety of the subsurface environment,  
44 ecosystem, and groundwater resources.

45 **Keywords:** geohydrologic parameters; seasonal changes; groundwater system; poroelastic  
46 response; precipitation

47

## 48 **1 Introduction**

49 Hydrogeological parameters are important parameters reflecting the hydrogeological  
50 characteristics of the groundwater system, which control the quality and quantity of groundwater  
51 resources in the crust. More and more studies have found that the geohydrologic parameters can  
52 be modified by earthquakes (e.g., Elkhoury et al., 2006; Liao et al., 2021; Shi et al., 2019; Zhang  
53 et al., 2019), and anthropogenic processes such as wastewater injection (Barbour et al., 2019;  
54 Fan et al., 2019; Wang et al., 2018). Even seasonal hydrological processes could change  
55 permeability, which is an important geohydrologic parameter, of groundwater system (Liang et  
56 al., 2022; Liao & Wang, 2018; Liao et al., 2022; Wang et al., 2019). However, the mechanism  
57 responsible for seasonal geohydrologic parameter variations during hydrological years remains  
58 an enigma.

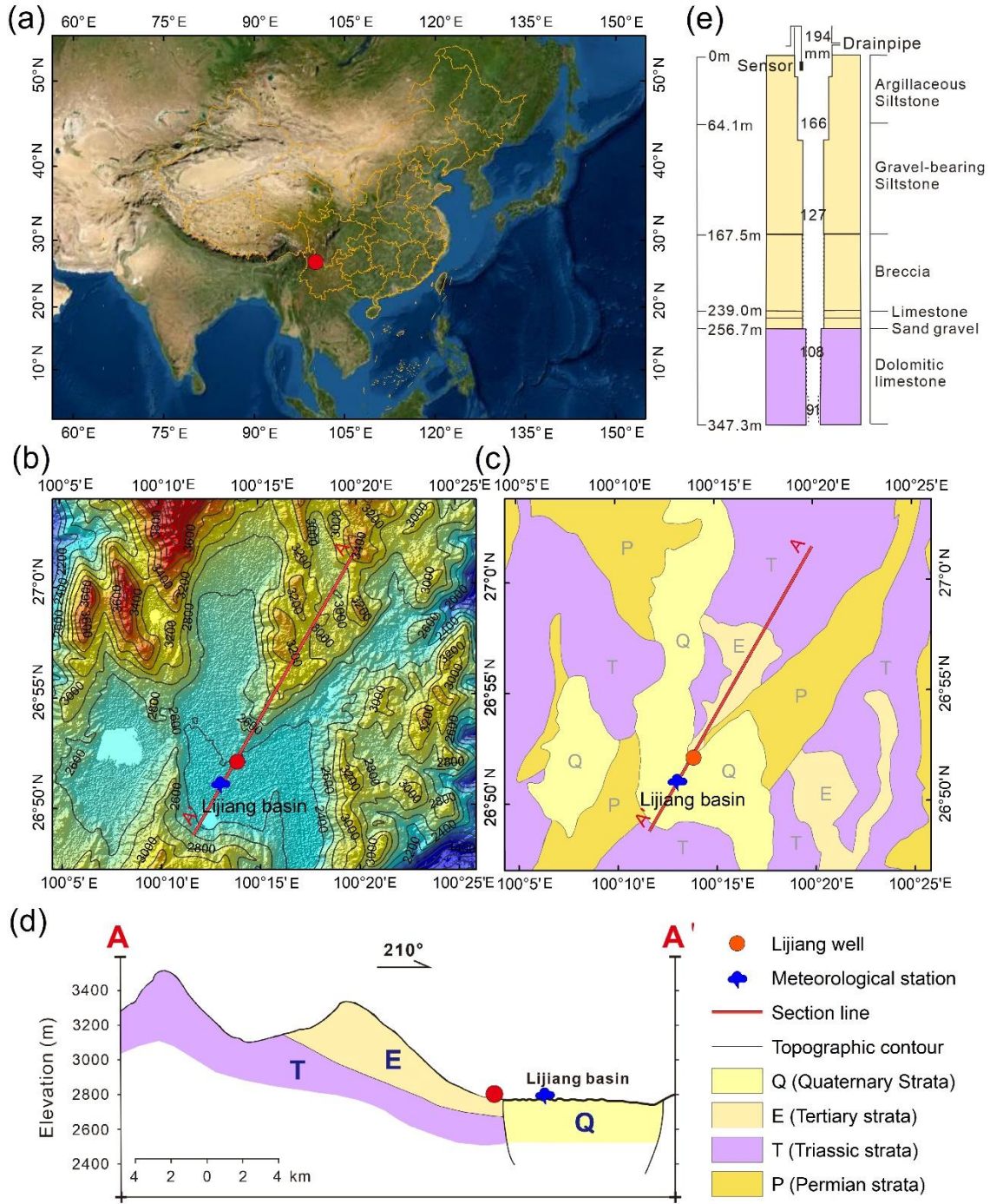
59           The tidal response method can be used effectively to study the geohydrologic parameters  
60 changes by utilizing continuous water level data from a groundwater well (Hsieh et al., 1987;  
61 Roeloffs, 1996; Wang et al., 2018). The advantages of the tidal response approach over other  
62 traditional methods, such as the pumping test, are the lower cost, the ability to monitor the  
63 geohydrologic parameters in real time, and the absence of disturbance to the aquifer (Xue et al.,  
64 2016). Consequently, this technique is widely employed to explore the effects of earthquakes,  
65 anthropogenic and hydrological processes on the geohydrologic parameters (e.g., Elkhoury et al.,  
66 2006; Liao & Wang, 2018; Liao et al., 2021, 2022; Wang et al., 2018; Shi et al., 2019).

67           To gain insights into the potential mechanism for seasonal geohydrologic parameter  
68 changes during hydrological years, we investigated the unexpected seasonal changes in the tidal  
69 response of the water level in the Lijiang well in Southwest China by employing an entirely new  
70 theoretical response model. The results show that the geohydrologic parameters may be  
71 connected with a seasonal change in the pore pressure of the aquifer. Based on this discovery, we  
72 proposed a new mechanism that may account for the seasonal variations in the geohydrologic  
73 parameters. Since the changes in geohydrologic parameters may control the storage and  
74 migration of groundwater and solutes, the present finding may have broad implications for  
75 understanding the safety of groundwater resources and the security of subsurface waste  
76 repositories during natural hydrological processes.

77

78 **2 Observations**

79           The Lijiang well (26°52'N, 100°14'E) was located in the northeastern part of the Lijiang  
80 Basin in Yunnan Province, Southwest China (**Figure 1a & 1b**). The subsurface geohydrology of  
81 the region consists of mid-Triassic carbonate rocks, which function as an aquifer and are  
82 partially covered by younger Tertiary sedimentary rocks (siltstone), which act as an aquitard (for  
83 detailed information see **Figures 1c, 1d & 1e**). The edge of the Lijiang Basin, in which the well  
84 is located, is the groundwater discharge area, which is regionally recharged by the precipitation  
85 from the mountains to the north of the basin (**Figure 1d**). The well is 347.3 m deep and revealed  
86 a carbonate aquifer at depths from 167.5 to 310 m, which is covered by a 167.5-meter thick  
87 siltstone aquitard (**Figure 1e**).

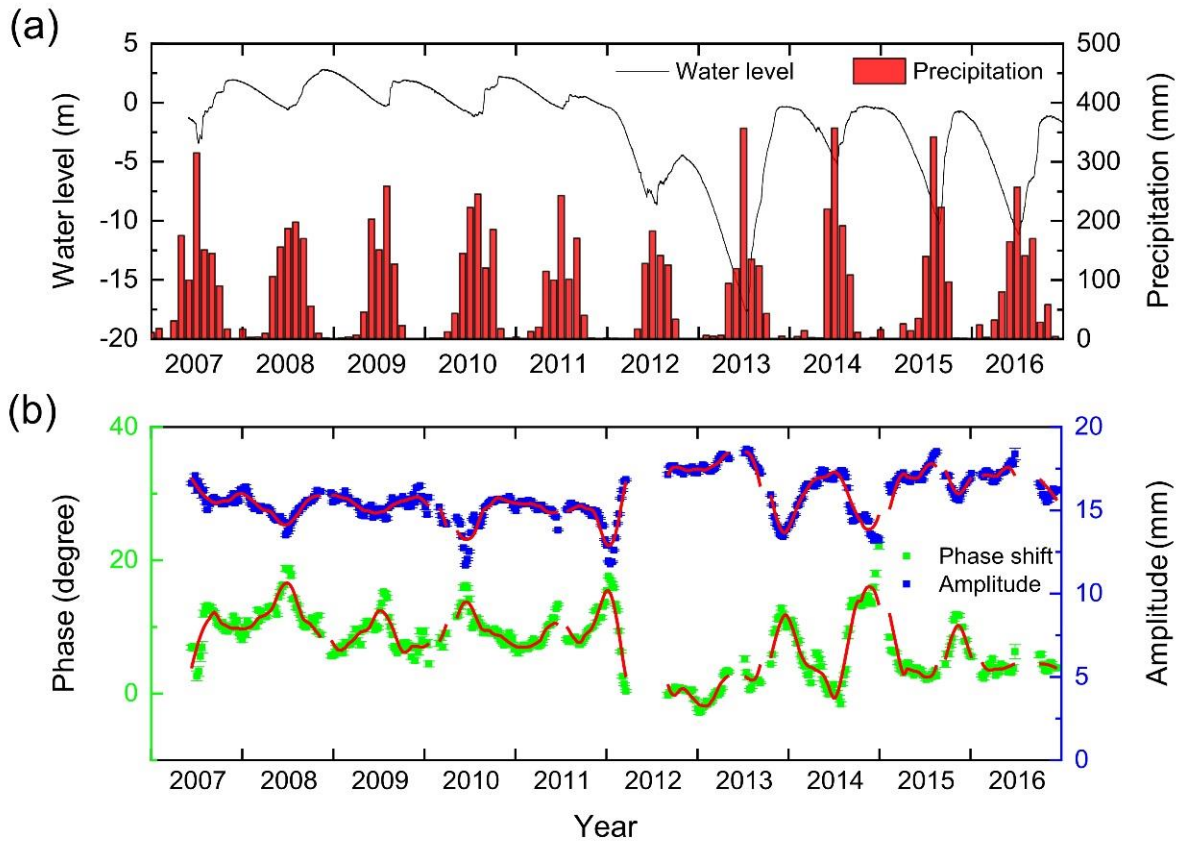


88

89 **Figure 1.** Overview of the observation well and its surrounding area. (a) The location map of the  
 90 Lijiang well and Lijiang meteorological station. The Lijiang meteorological station is to the  
 91 Southwest of the Lijiang well (about 2.5 km away). (b) Topography around the Lijiang well. (c)

92 Simplified hydrogeology around the Lijiang well. (d) Simplified cross-section of topography and  
93 hydrogeology around the Lijiang well. (e) Simplified diagram of the Lijiang well showing the  
94 lithology and the inner diameter of the well in mm. The dashed lines indicate the open section of  
95 the well.

96 **Figure 2a** shows water level data recorded in the Lijiang well from 2007 to 2016 and the  
97 local precipitation. This region experiences seasonal precipitation from June through September.  
98 The well water level annually rises from July to October and falls from November to June.  
99 Interestingly, the water levels do not respond to the local precipitation, implying that the aquifer  
100 is not hydraulically connected to the surface but is recharged at a distance from the well. **Figure**  
101 **2b** shows the changes in the amplitude and phase of the tidal response of the water level to the  
102 Earth tide. We employed the widely used Baytap-G routine (Tamura et al., 1991) for the tidal  
103 analysis, selected a 30-day window, and used the response to the semi-diurnal M2 lunar tide  
104 (Doan et al., 2006). Note that the amplitude and phase are negatively correlated and are related to  
105 the well water level (**Figure 2b**).



106

107 **Figure 2.** (a) The Lijiang well's water level and precipitation near the well over a ten-year  
 108 period. Excess water above the ground surface was drained through a drainpipe (**Figure 1e**). (b)  
 109 Amplitude and phase of the tidal response of the water level in the Lijiang well to the M2  
 110 (theoretical) tide plotted together with error bars as a function of time. The solid red line  
 111 represents the result of the amplitude and phase after smoothing.

### 112 3 Theoretical Model

113 Here, we briefly show the solution for the tidal response of a horizontally extensive leaky  
 114 confined aquifer to the Earth's tide (Wang et al., 2018). The aquifer is open to a well with a

115 radius of  $r_w$ , and the radius of the cased well is  $r_c$ . The phase shift ( $\eta$ ) and amplitude ratio ( $A$ ) of  
 116 tidal response of the water level in the well referenced to the tidal-strain equivalent head  $\left(\frac{BK_u \varepsilon_0}{\rho g}\right)$   
 117 are given by, respectively,

$$118 \quad A = \left| \frac{i\omega S}{(i\omega S + u)\xi} \right|, \quad (1)$$

$$119 \quad \eta = \arg \left[ \frac{i\omega S}{(i\omega S + u)\xi} \right]. \quad (2)$$

120 where,

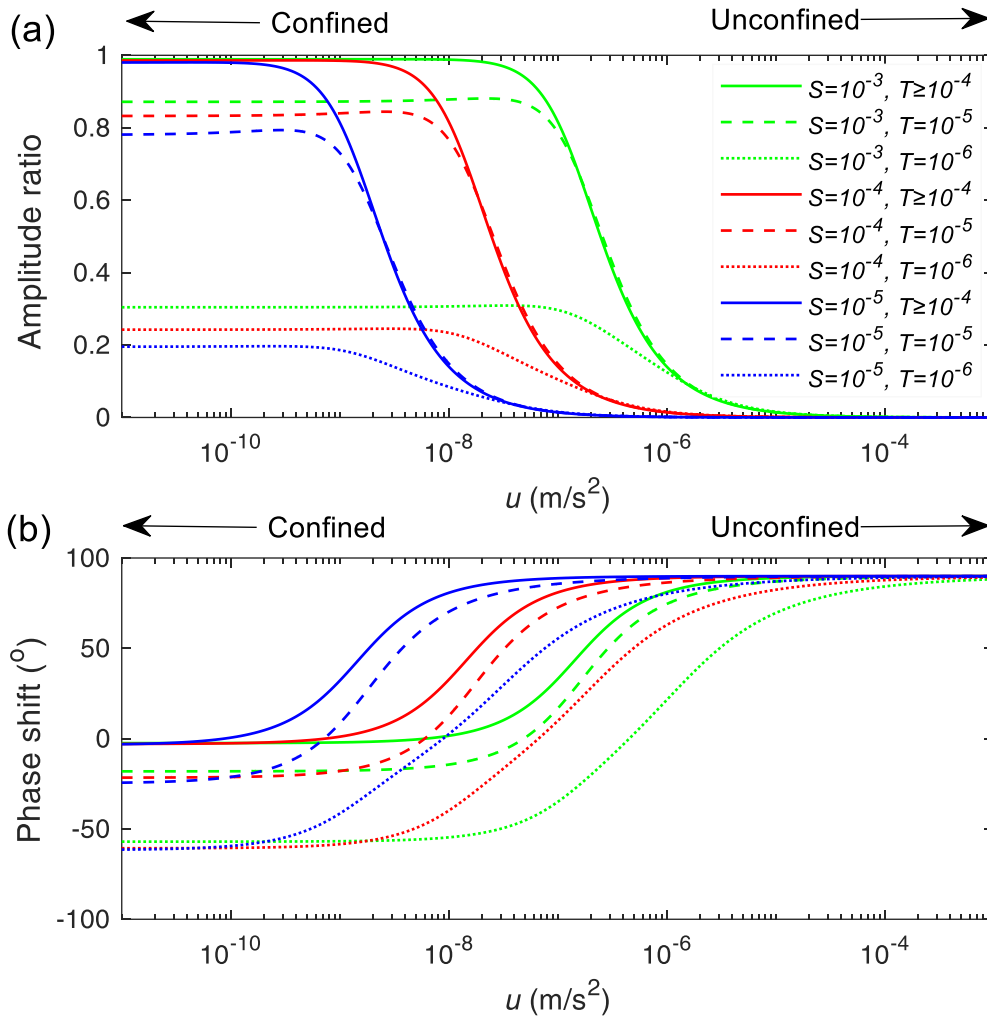
$$121 \quad \xi = 1 + \left(\frac{r_c}{r_w}\right)^2 \frac{i\omega r_w K_0(\beta r_w)}{2T\beta K_1(\beta r_w)}, \quad (3)$$

$$122 \quad \beta = \left(\frac{u + i\omega S}{T}\right)^{\frac{1}{2}}, \quad (4)$$

123  $B$ ,  $K_u$ ,  $\varepsilon_0$ , and  $\rho$  are the Skempton's coefficient, undrained bulk modulus, bulk strain, and  
 124 density, respectively, of the aquifer,  $g$  is the acceleration due to gravity,  $T = K * b$ ,  $u = K'/b'$ ,  
 125 and  $S$  are the transmissivity, leakage, and storativity, respectively, of the aquifer,  $K$  and  $b$  are  
 126 horizontal hydraulic conductivity and thickness, respectively, of the aquifer,  $K'$  and  $b'$  are the  
 127 vertical hydraulic conductivity and thickness, respectively, of the aquitard,  $\omega$  is angular  
 128 frequency of the water level tidal response to the Earth tide (for M2 tide,  $\omega = 1.9324 \text{ d}^{-1}$ ), and  
 129  $K_0$  and  $K_1$  are the modified Bessel function of the second kind of the 0th and the 1st order,  
 130 respectively.

131 For a given well, the amplitude ratio ( $A$ ) and phase shift ( $\eta$ ) of a specific tidal wave for  
 132 water level tidal response are related to the geohydrological parameters, including the storativity  
 133 ( $S$ ), transmissivity ( $T$ ), and leakage ( $u$ ) of the leaky confined aquifers. The analytical model for  
 134 the tidal response of the leaky confined aquifer described above, referred to here as the Wang et  
 135 al. (2018)'s model, also can be applied to estimate the hydrodynamic parameters of semi-

136 confined aquifers, as well as other different aquifer types, including unconfined aquifers and  
 137 confined ones. As shown in **Figure 3**, when the leakage is low enough, the semi-confined aquifer  
 138 acts as a confined aquifer, of which the tidal response is insensitive to the leakage changes (also  
 139 see Hsieh et al., 1987); while when the transmissivity is small enough, the semi-confined aquifer  
 140 acts as an unconfined aquifer, of which the tidal response is insensitive to the changes in  
 141 transmissivity (also see Roeloffs, 1996).



143 **Figure 3.** (a) Amplitude ratio and (b) phase shift of water level tidal response to the M2  
144 (semidiurnal lunar) tide, plotted against the leakage ( $u$ ) for different transmissivities ( $T$ ) and  
145 storativities ( $S$ ), with  $r_w = r_c = 10\text{cm}$ . Negative values of phase shift indicate phase lag.

#### 146 **4 Interpretation**

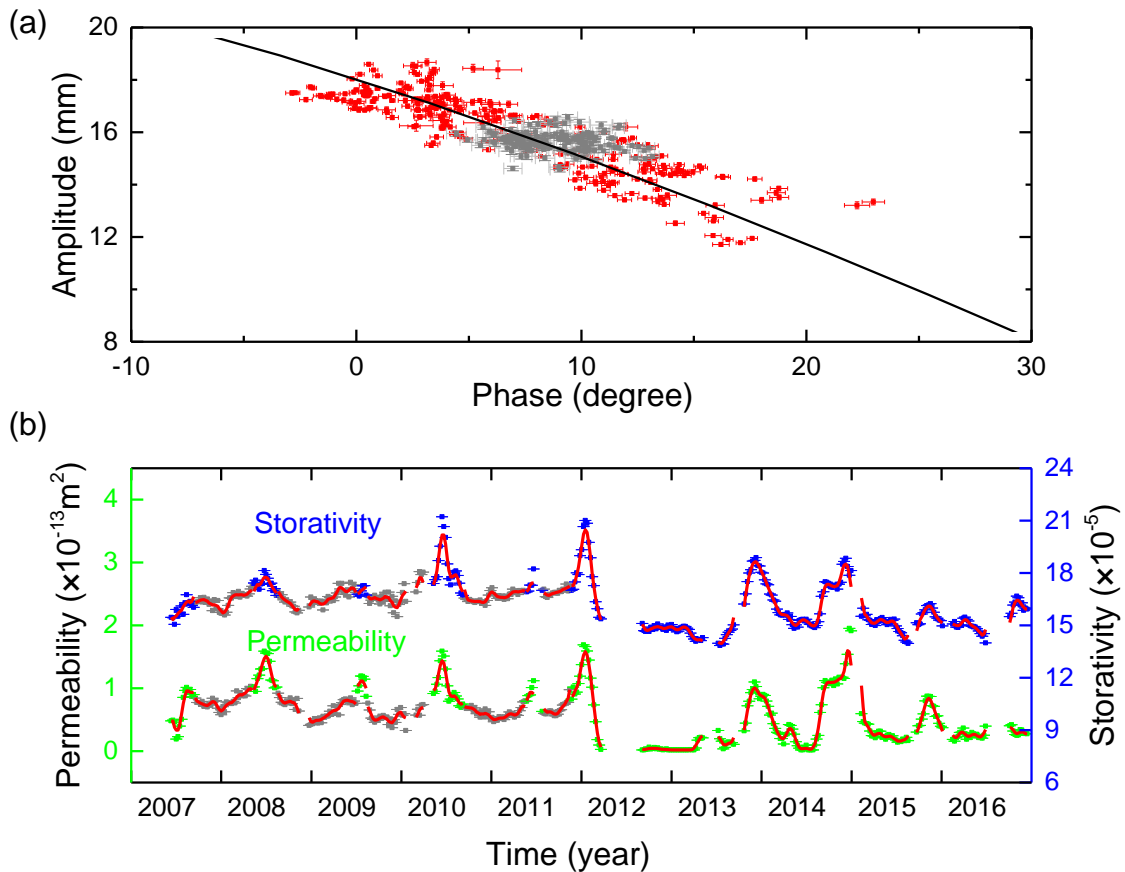
147 Wang et al. (2019) and Liang et al. (2022) analyzed, respectively, the possible effect of  
148 the capillary zone on the tidal response of the water level in the Lijiang well using numerical  
149 simulations and analytical model, and attributed the variations in the tidal response of the water  
150 level to the impact of the capillary zone. However, their simulation assumes that the observed  
151 aquifer is unconfined (despite of the fact that it is a semi-confined or a leaky aquifer, see **Figure**  
152 **1d & 1e**), indicating that the capillary effect on the water level tidal response may be  
153 considerably overestimated. Zhu (2022) then discussed the capillary effect of semi-confined  
154 aquifer on the tidal response of water level in Lijiang well through numerical simulation.  
155 Although her complex numerical models could fit the correlation between amplitude (ratio) and  
156 phase (shift), the reliability of fitting results was insufficient to explain the seasonal changes in  
157 the tidal response of water level because there are no actual geohydrological parameter values  
158 used during the fitting. Moreover, the actual process of tidal response of well water level without  
159 capillary hysteresis (see **Figure 4a & 5**) is inconsistent with the tidal response caused by  
160 capillary effect which shows that there are differences between the tidal response during the  
161 rising of water level and that during the falling of water level (see **Figure 4b** in Liao et al.,

162 2022), which indicates that the seasonal changes in tidal response is not caused by the seasonal  
163 changes in capillary action.

164 Liao and Wang (2018) used Roeloffs (1996)'s tidal response model for an unconfined  
165 aquifer to explain the changes in the tidal response of the well water level. They attributed the  
166 changes in the tidal response to the changes in the vertical permeability of the unconfined  
167 aquifer. Nevertheless, based on the geohydrological setting (**Figure 1c & 1d**) and the fact that  
168 the amplitude and phase are inversely proportional (**Figure 4a**), we concluded that the aquifer  
169 observed by the Lijiang well is a semi-confined or leaky confined aquifer. Therefore, we  
170 employed Wang et al. (2018)'s theoretical model to explain the tidal response of water level in  
171 the Lijiang well. As shown in **Figure 4a**, the amplitude and phase can be fitted with Wang et al.  
172 (2018)'s model, indicating that the tidal response of the water level in the Lijiang well can be  
173 explained by the tidal response model of a leaky confined aquifer.

174 Based on the tidal response model of a leaky confined aquifer (see **Theoretical Model**;  
175 Wang et al., 2018), we were able to estimate the vertical permeability ( $k'$ ) of the aquitard and the  
176 storativity ( $S$ ) of the aquifer during the study period using the amplitude (or amplitude ratio) and  
177 phase (or phase shift) of the tidal response of the well water level (see **Figure 4b**). As shown in  
178 **Figure 4b**, the vertical permeability and storativity are positively correlated and change  
179 seasonally. The vertical permeability and storativity decreased synchronously between July and  
180 October (during the rainy season) and increased synchronously between November and June  
181 (during the dry season). In our study, the horizontal permeability or transmissivity of the aquifer

182 cannot be estimated because the amplitude ratio and phase shift are insensitive to changes in the  
183 transmissivity at high transmissivity ( $T_h \sim 10^{-1} \text{m}^2/\text{s}$ ; refer to Liao and Wang (2018) who  
184 estimated the transmissivity by using the seasonal response of water level to the precipitation)  
185 (see **Figure 3**).



186

187 **Figure 4.** (a) Actual and theoretic correlation between the amplitude and phase of the M2 tide of  
188 the water level. The scatter plot was generated using water level data recorded in the Lijiang  
189 well; and the theoretical curves were obtained using Wang et al. (2018)'s theoretical model by  
190 setting  $T = 10^{-1} \text{m}^2/\text{s}$  (refer to Liao and Wang, 2018). The gray dots represent the amplitude  
191 and phase under drainage conditions that were not analyzed further, as the well water drainage

192 has effect on the tidal response of the well water level. **(b)** Vertical permeability ( $k'$ ) of the  
193 aquitard and storativity ( $S$ ) of the aquifer over time with error bars by using Wang et al. (2018)'s  
194 theoretical model. The solid red line represents the vertical permeability and storativity after  
195 smoothing. Note that the estimated values of the vertical permeability and storativity differed  
196 significantly (by an order of magnitude) from those reported by Liao and Wang (2018), who  
197 used an unconfined aquifer model.

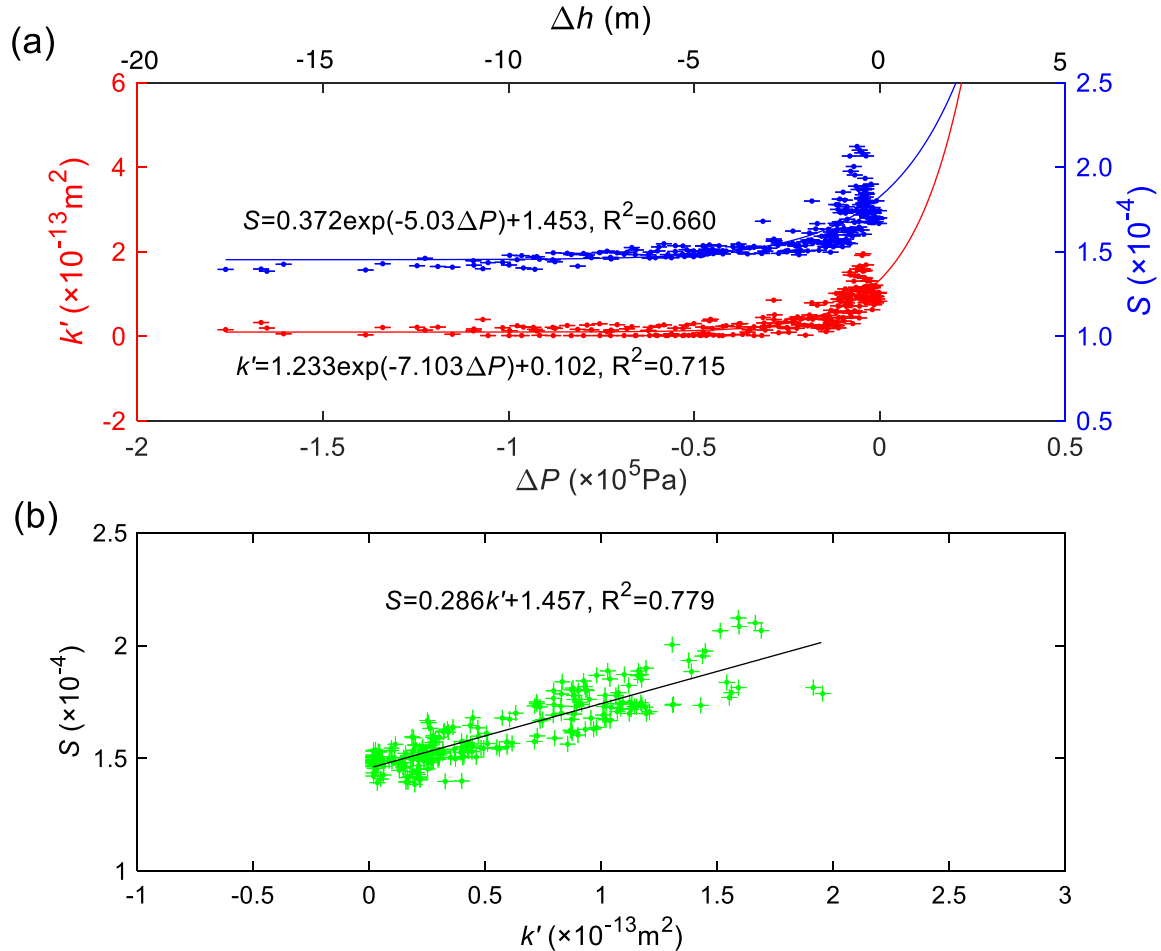
198

## 199 **5 Discussion**

200         Given that the vertical permeability is positively correlated with the well water level or  
201 pore pressure in the groundwater system, Liao and Wang (2018) argued that the clogging and  
202 unclogging of fractures induced by changes in the pore pressure is responsible for the seasonal  
203 changes in vertical permeability. The changes in vertical permeability caused by the  
204 aforementioned mechanism tend to lag behind the changes in well water level or pore pressure  
205 because the process of fracture clogging and unclogging takes time. However, the field data does  
206 not support this mechanism, as no lag loop was observed between the vertical permeability &  
207 storativity and the well water level or pore pressure, which suggests that the seasonal response of  
208 the geohydrologic parameters to the hydrologic process is immediate and nonhysteretic (see  
209 **Figure 4**). Therefore, a plausible new mechanism is required to explain the observed fluctuations  
210 in both the amplitude (ratio) and phase (shift) of the tidal response of the well water level.

211 **Figure 5** shows the correlation between the hydrogeological parameters, including the  
212 vertical permeability ( $k'$ ), the storativity ( $S$ ), and the change in pore pressure ( $\Delta P$ ) or well water  
213 level ( $\Delta h$ ). The fitting relationship between hydrogeological parameters and pore pressure  
214 demonstrated by on-site observation data is the same as the empirical one proposed by Raghavan  
215 and Chin (2004) to determine the permeability of pore pressure or stress sensitive fractured  
216 aquifers during the poroelastic response process. The exponential relationships between vertical  
217 permeability and storativity and pore pressure indicate that the seasonal response of the  
218 groundwater system is significantly dependent on pore pressure or effective stress of the  
219 groundwater system, implying that the geohydrologic parameters of the groundwater system are  
220 extremely sensitive to pore pressure changes. In addition, the vertical permeability and storativity

221 are linearly correlated with each other, which implies that the same mechanism should be  
 222 responsible for the changes in both quantities during the response process.



223  
 224 **Figure 5.** (a) Correlation between the storativity ( $S$ ) or the vertical permeability ( $k'$ ) and the  
 225 change in pore pressure ( $\Delta P$ ) or well water level ( $\Delta h$ ). (b) Correlation between the storativity ( $S$ )  
 226 and the vertical permeability ( $k'$ ). The water level was averaged over a 30-day period. The pore  
 227 pressure ( $P$ ) was calculated using  $P = \rho g h$ , where  $\rho = 10^3 \text{kg/m}^3$  is the density of the  
 228 groundwater,  $g = 9.8 \text{m/s}^2$  is the acceleration due to gravity, and  $h$  is the well water level. The  
 229 best fit of the correlation between the vertical permeability ( $k'$ ) and the changes in pore pressure

230  $(\Delta P)$  is  $k' = k'_0 e^{-d\Delta P} + k'_1$ , where  $d = 7.103 \times 10^{-5} \text{Pa}^{-1}$  is the characteristic parameter of the  
231 rock mass,  $k'_0 = 1.233 \times 10^{-13} \text{m}^2$  is the “initial” permeability when the pore pressure is  
232 sufficiently high,  $k'_1 = 0.102 \times 10^{-13} \text{m}^2$  is the “residual” permeability when the pore pressure  
233 is low enough. The best fit of the correlation between the storativity ( $S$ ) and the changes in pore  
234 pressure ( $\Delta P$ ) is  $S = S_0 e^{-d'\Delta P} + S_1$ , where  $d' = 5.030 \times 10^{-4} \text{Pa}^{-1}$  is the characteristic  
235 parameter of the rock mass,  $S_0 = 0.372 \times 10^{-4}$  is the “initial” storativity when the pore pressure  
236 is sufficiently high, and  $S_1 = 1.453 \times 10^{-4}$  is the “residual” storativity when the pore pressure  
237 is low enough.

238

239         Based on the nonhysteretic exponential correlation with the pore pressure, the seasonal  
240 changes in vertical permeability and storativity can be attributed to the poroelastic response in  
241 the fracture aperture caused by the seasonal changes in the pore pressure or effective stress of the  
242 groundwater system, rather than the fracture unclogging/clogging proposed by Liao & Wang  
243 (2018). Increases in pore pressure result in an increase in the fracture aperture, which in turn  
244 leads to an increase in the vertical permeability and storativity. On the other hand, as the pore  
245 pressure decreases, the fracture aperture decreases, lowering the vertical permeability and  
246 storativity. A change in the fracture aperture caused by a change in pore pressure is a poroelastic  
247 response and usually doesn't take time; therefore, the vertical permeability, storativity, and pore  
248 pressure changes occur almost simultaneously, which is consistent with observations from the  
249 Lijiang Well (see Figure 4 & 5).

250         We proposed a novel potential mechanism to explain the seasonal vertical permeability

251 and storativity changes. These seasonal changes can be attributed to seasonal fracture aperture  
252 changes or seasonal fractures opening/closing in the groundwater system, which are caused by  
253 regional rainfall recharge inducing changes in pore pressure or effective stress during a  
254 hydrologic year. The cyclic seasonal changes in the vertical permeability and storativity also  
255 suggest a reversible poroelastic process throughout a hydrological year. Because of this regional  
256 precipitation recharge, the pore pressure of the groundwater system will increase, leading to  
257 increases in the fracture apertures, vertical permeability, and storativity. In contrast, as the pore  
258 pressure decreases, the vertical permeability and storativity will recover to their pre-recharge  
259 level.

260           It has been suggested that seasonal hydrologic processes can reshape groundwater  
261 systems through seasonal variations in geohydrologic parameters, thereby affecting the seasonal  
262 hydrologic response in subsurface systems. Recharging groundwater makes the groundwater  
263 system more permeable and storable during the rainy season. Therefore, the groundwater is a  
264 linked poroelastic–hydraulic system with positive feedback. The feedback may have a seasonal  
265 effect on the subsurface ecosystems and environments, such as groundwater security, the safety  
266 of nuclear waste storage, and diffusion and transport of pollutants, increasing the risks associated  
267 with a number of ecological and environmental issues in the subsurface system.

268

## 269 **6 Conclusions**

270 In this study, motivated by the fact that changes in the vertical permeability and storativity  
271 of the groundwater system occurred almost simultaneously with the changes in the pore pressure,  
272 as seen by the Lijiang well, we proposed a new mechanism to explain the seasonal pore pressure  
273 dependent geohydrologic parameter fluctuations inferred from the tidal response of the water  
274 level in the Lijiang well. We attributed the seasonal geohydrologic parameter fluctuations to the  
275 fracture aperture changes or the opening/closing of pre-existing fractures in the groundwater  
276 system that resulted from the pore pressure perturbation-induced poroelastic response of the  
277 groundwater system. Such seasonal geohydrologic parameter changes are expected to alter  
278 groundwater storage, flow patterns, and transport processes in the groundwater system during a  
279 rainy season. Considering that these processes may impact the migration of contaminants and the  
280 security of subsurface waste repositories, the findings of this study may have far-reaching  
281 implications for the safety of the subsurface environment, ecosystem, and groundwater  
282 resources.

283

## 284 **Acknowledgments**

285 The work was supported by Spark Program of Earthquake Science (XH23063A),  
286 Fundamental Research Funds for the Central Universities of China (ZY20215104), National  
287 Natural Science Foundation (41602274), and Scientific Research Project of Three Gorges Group  
288 Corporation (0799217). We thank Zhu-Zhuan Yang and Xiao-Jing Hu for the help with data

289 collection, Ai-Yu Zhu and Lili Zhang for their helpful suggestions, Xiong Zhang and Wei Liao  
290 for their help with the creation of graphs, the China Earthquake Datacenter for providing the well  
291 water level data, and the China Meteorological Administration for providing the precipitation  
292 data.

### 293 **Data Availability Statement**

294 Well-water level data may be downloaded through an application of China Earthquake  
295 Networks Center, National Earthquake Data Center (URL:  
296 <https://data.earthquake.cn/datashare/login.jsp>). Precipitation data may be downloaded through an  
297 application of China Meteorological Data Service Centre, China Meteorological Administration  
298 (URL: <http://data.cma.cn/data/cdcindex/cid/0b9164954813c573.html>).

299

### 300 **References**

- 301 Barbour, A. J., Xue, L., Roeloffs, E., & Rubinstein, J. L. (2019). Leakage and increasing fluid  
302 pressure detected in Oklahoma's waste water disposal reservoir. *Journal of Geophysical*  
303 *Research: Solid Earth*, 124(3), 2896–2919. <https://doi.org/10.1029/2019JB017327>.
- 304 Doan, M. L., Brodsky, E. E., Prioul, R., & Signier, C. (2006). Tidal analysis of borehole  
305 pressure: A tutorial, Schlumberger-Doll Research Report, (Available at  
306 [https://isterre.fr/IMG/pdf/tidal\\_tutorial\\_SDR.pdf](https://isterre.fr/IMG/pdf/tidal_tutorial_SDR.pdf). Cambridge, Massachusetts.
- 307 Elkhoury, J. E., Brodsky, E. E., & Agnew, D. C. (2006). Seismic waves increase permeability.

- 308 Nature, 441(7097), 1135–1138. doi:10.1038/nature04798.
- 309 Fan, Z., Eichhubl, P., & Newell, P. (2019). Basement fault reactivation by fluid injection into  
310 sedimentary reservoirs: Poroelastic effects. *Journal of Geophysical Research: Solid Earth*,  
311 124, 7354– 7369. doi:10.1029/2018JB017062.
- 312 Hsieh, P. A., Bredehoeft, J. D., and Farr, J. M. (1987), Determination of aquifer transmissivity  
313 from Earth tide analysis, *Water Resour. Res.*, 23( 10), 1824– 1832,  
314 doi:10.1029/WR023i010p01824.
- 315 Liang, X.Y., Wang, C.-Y., Ma, E.Z., & Zhang, Y.-K., (2022). Effects of unsaturated flow on  
316 hydraulic head response to Earth tides—An analytical model. *Water Resources Research*, 58,  
317 e2021WR030337. <https://doi.org/10.1029/2021WR030337>.
- 318 Liao, X., Wang, C.-Y., Wang, Z.-Y. (2022). Seasonal change of groundwater response to Earth  
319 tides, *Journal of Hydrology*, 615(Part A), 128118.  
320 <https://doi.org/10.1016/j.jhydrol.2022.128118>.
- 321 Liao, X., Shi, Y., Liu, C.-P., & Wang, G. (2021). Sensitivity of permeability changes to different  
322 earthquakes in a fault zone: Possible evidence of dependence on the frequency of seismic  
323 waves. *Geophysical Research Letters*, 48, e2021GL092553.  
324 <https://doi.org/10.1029/2021GL092553>
- 325 Liao, X., & Wang, C.-Y. (2018). Seasonal permeability change of the shallow crust inferred  
326 from deep well monitoring. *Geophysical Research Letters*, 45(20), 130–111, 136.  
327 <https://doi.org/10.1029/2018GL080161>.
- 328 Raghavan, R., & Chin, L. Y. (2004). Productivity changes in reservoirs with stress-dependent

- 329 permeability. *SPE Reservoir Evaluation & Engineering*, 7(4), 308–315.
- 330 Roeloffs, A. (1996). Poroelastic techniques in the study of earthquake-related hydrology  
331 phenomenon. *Advances in Geophysics*, 37, 135–195.
- 332 Shi, Y., Liao, X., Zhang, D., & Liu, C.-P. (2019). Seismic waves could decrease the permeability  
333 of the shallow crust. *Geophysical Research Letters*, 46(12), 6371–6377.  
334 <https://doi.org/10.1029/2019GL081974>.
- 335 Tamura, Y., Sato, T., Ooe, M., & Ishiguro, M. (1991). A procedure for tidal analysis with a  
336 Bayesian information criterion. *Geophysical Journal International*, 104(3), 507–516.
- 337 Wang, C.-Y., Doan, M.-L., Xue, L., & Barbour, A. J. (2018). Tidal response of groundwater in a  
338 leaky aquifer — Application to Oklahoma. *Water Resources Research*, 54(10), 8019–8033.  
339 <https://doi.org/10.1029/2018WR022793>.
- 340 Wang, C.-Y., Zhu, A.-Y., Liao, X., Manga, M., & Wang, L.-P. (2019). Capillary effects on  
341 groundwater response to earth tides. *Water Resources Research*, 55(8), 6886–6895.
- 342 Xue, L., Brodsky, E. E., Erskine, J., Fulton, P. M., & Carter, R. (2016). A permeability and  
343 compliance contrast measured hydrogeologically on the San Andreas Fault. *Geochemistry,  
344 Geophysics, Geosystems*, 17(3), 858–871. doi:10.1002/2015GC006167.
- 345 Zhang, H., Shi, Z., Wang, G., Sun, X., Yan, R., & Liu, C. (2019). Large earthquake reshapes the  
346 groundwater flow system: Insight from the water-level response to earth tides and  
347 atmospheric pressure in a deep well. *Water Resources Research*, 55(5), 4207–4219.  
348 doi:10.1029/2018WR024608.
- 349 Zhu Ai-Yu. (2022). *Unsaturated Flow Influences the Response of Leaky Aquifer to Earth Tides*.

